



Draft Manuscript for Review

Repeatability of Renal Arterial Spin Labelling MRI in Healthy Subjects

Journal:	<i>MAGMA Magnetic Resonance Materials in Physics, Biology and Medicine</i>
Manuscript ID:	MAGMA-11-0073.R2
Manuscript Type:	Original
Date Submitted by the Author:	n/a
Complete List of Authors:	Cutajar, Marica; UCL Institute of Child Health, Imaging and Biophysics Thomas, David; UCL Institute of Neurology, Department of Brain Repair and Rehabilitation Banks, Tina; Great Ormond Street Hospital, Radiology Department Clark, Christopher; UCL Institute of Child Health, Imaging and Biophysics Golay, Xavier; UCL Institute of Neurology, Department of Brain Repair and Rehabilitation Gordon, Isky; UCL Institute of Child Health, Imaging and Biophysics
Keywords:	Arterial Spin Labelling, Renal Perfusion, Repeatability , 3D GRASE

SCHOLARONE™
Manuscripts

Repeatability of Renal Arterial Spin Labelling MRI in Healthy Subjects

M. Cutajar^{1*}, D. L. Thomas^{2*}, T. Banks³, C. A. Clark¹, X. Golay², and I. Gordon¹

* joint first authors

¹Imaging and Biophysics Unit, UCL Institute of Child Health, 30 Guilford Street, London WC1N 1EH, UK

²Department of Brain Repair and Rehabilitation, UCL Institute of Neurology, Queen Square, London WC1N 3BG, UK

³Department of Radiology, Great Ormond Street Hospital, London WC1N 3JH, UK

Communicating authors:

Marica Cutajar: m.cutajar@ucl.ac.uk
+44 20 7905 2300 (tel)
+44 20 7905 2358 (fax)

David Thomas: d.thomas@ucl.ac.uk
+44 20 3448 4409 (tel)
+44 20 3448 4413 (fax)

Abstract word count: 231

Main text word count: 3728

Number of figures: 6

Number of tables: 2

Number of references: 36

Abstract:

Object: Arterial Spin Labelling (ASL) can be used to measure renal perfusion non-invasively. The aim of this study was to determine the repeatability of this technique in healthy kidneys to vindicate its use in clinic.

Materials and Methods: Two groups of healthy volunteers were imaged two different days to assess intra- and inter-session repeatability. Oblique-coronal data volumes were acquired on a 1.5 T scanner with a dedicated abdominal 32 channel body phased array coil. ASL was performed using a multi-TI FAIR labelling scheme and 3D GRASE imaging module. Background suppression and respiratory triggering were used. T₁ maps of the kidney were acquired using the same sequence with background suppression disabled.

Results: For the group with multiple intra-session ASL measurements, the average cortical perfusion was 197 mL/min/100g and average cortical T₁ was 1265ms. For both perfusion and T₁ the variation shown by the within-subject standard deviation (SDws) (14.6 mL/min/100g and 33.4 ms) and coefficient of variation (CVws) (7.52% and 2.69% respectively) was small for all the analyses carried out. Bland-Altman plots were also used to visualise the variation between the same parameters collected from the different scanning sessions in both groups, and demonstrated good reproducibility.

Conclusion: We have shown that in healthy volunteers, ASL parameters are repeatable over a short and long period. This supports the overall aim of using ASL in the clinic to assess longitudinal renal perfusion changes in patients.

Keywords:

Arterial Spin Labelling, Renal Perfusion, Repeatability, 3D GRASE

Introduction:

A major function of the kidney is filtration, which is crucially dependent on renal perfusion. Quantitative assessment of renal perfusion rate can provide valuable insight and possibly early diagnosis following renal transplantation (1, 2). In the clinical setting, while radionuclide scintigraphy is the commonest method used to assess renal perfusion, it is semi-quantitative and only provides an index of perfusion, as opposed to quantitative blood flow rate. Furthermore it requires the injection of a radioactive tracer, making it an invasive technique (3, 4). Quantitative values can be obtained from Positron Emission Tomography (PET), but this is invasive as it requires arterial blood sampling. X-ray Computed Tomography can also be used, but at the expense of a high radiation burden which is unacceptable to most clinicians. There is therefore no current technique widely available to measure renal perfusion non-invasively. However, Arterial Spin Labelling (ASL) is an MRI technique that offers a rapid and non-invasive method to provide a quantitative measure of perfusion in an organ of interest (5-8).

Perfusion contrast in the ASL images comes from the calculation of the difference between two successively acquired images. The two images differ in that one is acquired with and one without the labelling of the arterial water spins, followed by a time interval (TI). The first clinical renal ASL papers were published in the mid-late 1990s (9, 10). Since then, a range of studies have been performed which have tried to improve the method for application to the kidney. In particular, fast imaging techniques which are suitable for abdominal imaging have been applied, such as true fast imaging with steady-state precession (TrueFISP) and fast spin echo/ultra-fast low-angle rapid acquisition and relaxation enhancement (UFLARE) (11-16). While these techniques result in good image quality, they suffer from limited volume coverage (often just a single slice). In addition to measuring perfusion in the normal kidney, several studies have investigated the effect of different diseases on kidney perfusion, including renal cell carcinoma and renal artery stenosis, as well as monitoring blood flow levels in transplanted kidneys (14, 15, 17). Most previous studies have acquired ASL images using a single TI, and have used a basic blood flow quantification model that assumes arterial transit times to be negligible (18). Recently, more sophisticated acquisition schemes have been applied which either use a single TI approach made insensitive to transit time (QUIPSS II with thin-slice $T_{1\rho}$ periodic saturation (Q2TIPS) (19), where QUIPSS II is quantitative imaging of perfusion using a single subtraction, version II (20)) or use a range of TI values (21) and so measure transit times by fitting the series of images to the general kinetic ASL model (22). In diseased and transplanted kidneys, these more advanced ASL

1
2
3 techniques are likely to produce much more robust estimates of tissue
4 perfusion. The use of image acquisition methods which permit the acquisition
5 of multi-slice data sets has recently been investigated (23), providing more
6 extensive volumetric information.
7
8

9
10 When multi-TI acquisitions are performed, analysis of the raw ASL data
11 allows four parameters to be extracted: perfusion ($\text{mL min}^{-1} 100 \text{ g}^{-1}$ of tissue),
12 arterial transit time Δt (ms), longitudinal relaxation time T_1 (ms) and
13 equilibrium magnetisation M_0 values. T_1 and M_0 maps can be calculated using
14 the ASL sequence without background suppression (24). The imaging volume
15 is subjected to a saturation pulse prior to the spin labelling sequence and
16 hence the data are treated in the same way as that obtained from a saturation
17 recovery experiment (25). Calculation of the perfusion and Δt maps can then
18 be computed from a separately acquired background-suppressed ASL data set
19 using the Buxton general kinetic model (22). In a healthy kidney, renal blood
20 flow is approximately $1.1 \text{ litre min}^{-1}$ (26), which can be expressed as
21 approximately $240 \text{ mL min}^{-1} 100 \text{ g}^{-1}$ of tissue if the standard kidney volume is
22 assumed to be around 230 mL (27).
23
24
25
26
27
28

29
30 In this study, we used a multi-TI pulsed ASL approach in combination with a
31 background-suppressed 3D GRASE image acquisition module (24). To
32 establish the potential of this as a clinically feasible technique for measuring
33 renal perfusion, we determined the repeatability (standard deviation and
34 coefficient of variation) of the kidney blood flow measurements in two groups
35 of subjects scanned at different time points, within and across different
36 scanning sessions.
37
38
39
40
41
42
43
44
45
46
47
48
49
50
51
52
53
54
55
56
57
58
59
60

Materials and Methods:

This study was approved by the local ethics committee. Two groups of subjects were scanned (group A and group B). Group A (five healthy volunteers: age range 29 – 67 years, median = 30 years) were scanned on two separate occasions (8 – 174 days apart; median = 21 days) using identical scanning protocols. TrueFISP images were acquired in 3 orientations (axial, coronal and sagittal) to establish the position of the main arteries and kidneys prior to setting up the ASL. On each occasion the ASL sequence was acquired three times successively. Groups B (twenty healthy volunteers: age range 22 – 40 years, median = 31 years) underwent the same procedure except that only a single ASL measurement was made on each occasion (7 – 55 days apart; mean time between sessions = 17.6 days; median = 7 days). Volunteers were asked to relax and breathe normally throughout the data acquisition as respiratory triggering was used to minimise motion effects in the ASL images.

ASL data volumes were acquired on all volunteers on a 1.5 T Siemens Avanto scanner (Siemens Healthcare, Erlangen, Germany) with a dedicated abdominal TIM 32 channel body phased array coil. The body matrix and six elements of the inbuilt spine matrix were used for signal reception. ASL was performed using a multi-TI pulsed ASL acquisition, with a FAIR labelling scheme and segmented 3D GRASE imaging module (24) preceded by a volume-selective saturation pulse and background suppression scheme (28) (see Figure 1(a)). Coronal oblique slices were acquired to minimize in-plane kidney motion (Figure 1(b)). In order to acquire images with a sufficient range of TI values to accurately sample the inflow curve while keeping to a reasonable scan time, single average images were acquired. Fourteen TI values were used, following both selective and non-selective inversion, ranging from 100ms to 2700ms with 200ms spacing. This allowed simultaneous assessment of arterial transit times and renal perfusion, via fitting to the standard ASL kinetic model. TR was 3000 ms and TE was 28ms. Please note that TR did not have to be changed in this particular implementation because of the presence of the pre-saturation pulse. The voxel size was $3.1 \times 3.1 \times 5.0 \text{ mm}^3$ with a matrix size of $128 \times 104 \times 12$ and sampling bandwidth of 217 kHz. A fat saturation pulse was applied immediately before image acquisition. Partial Fourier sampling was applied along the second phase encoding direction (partial Fourier factor 3/4) and the acquisition was spilt into three segments, with segmentation performed in the frequency encoding direction. The first refocusing pulse had a nominal flip angle of 180° , followed by a train of 130° pulses (to prolong the lifetime of available signal). The total GRASE acquisition period for each segment (including data sampling and refocusing pulses) was 244ms. Background suppression and respiratory triggering were used to maximise measurement precision. Background suppression consisted of a pre-saturation pulse (applied directly

1
2
3 after the ASL labelling pulse) followed by two adiabatic inversion pulses
4 during the inflow time T_I , with inversion times chosen to null tissues with T_1
5 values of 700ms and 1400ms (according to the scheme described by Gunther
6 et al. (24)). Prospective respiratory gating using bellows was performed,
7 which triggered the application of the labelling pulse. The slice thickness of
8 the slice-selective FAIR inversion pulse was also 60mm, and it was ensured
9 that the aorta was not in the proximity of the selective inversion pulses *i.e.*
10 outside the prescribed imaging volume (see Figure 1(b)). The acquisition time
11 for one ASL run was 4 min 12sec. T_1 and M_0 maps of the kidney (required for
12 perfusion quantification) were acquired using the same sequence with
13 background suppression disabled, according to (24).
14
15

16
17
18
19 The ASL images were imported onto a PC and analysed using a home written
20 program (Matlab R2010b (The MathWorks, Inc.)). The program first
21 computed the M_0 and T_1 map by fitting to the saturation recovery formula
22 derived from the Bloch equations ($M_z = M_0(1 - \exp(-T_I/T_1))$, where M_z is the z-
23 magnetization at time point T_I) to each pixel in the image. The resulting M_0
24 and T_1 values were entered into the Buxton kinetic model where they were
25 used with the ASL data to generate perfusion and arterial transit time maps
26 on a pixel-by-pixel basis.
27
28

29
30 Two central slices of each kidney were identified, and cortical and whole
31 kidney regions of interest (ROI) were drawn on the raw non-background
32 suppressed images using a home written program (Matlab R2010b (The
33 MathWorks, Inc.)). The ROIs were then transferred onto the perfusion, T_1 and
34 arterial transit time parameter maps to extract their respective values.
35
36
37

38 39 **Statistics:**

40
41 This study analysis is in two parts. The first part of the study, or 'short-term
42 repeatability study', examined the three repeats carried out on the same day
43 (Group A 10 kidneys (5 left and 5 right), 30 data sets in total (Tables 1a and
44 b)). A one-way (single factor) ANOVA was used to calculate the mean within-
45 subject variance, from which the within-subject standard deviation was
46 calculated ($SD_{ws} = \sqrt{\text{Variance}_{ws}}$) (29). The within-subject coefficient of variation
47 (CV_{ws}) was calculated using SD_{ws} together with the mean of the mean
48 obtained from each of the three repeats.
49
50

51
52 The second analysis (*i.e.* first scan versus second scan) assessed the
53 repeatability of the technique over a longer period of time, hence 'long-term
54 study'. For group A, the averaged data from the 3 acquisitions performed on
55 each of the 5 volunteers on each of the two scanning sessions were used to
56 make a direct comparison of each individual's results on the two scanning
57 days. Repeatability was assessed using a Bland-Altman plot (30). This was
58 used to visualise the dispersion of perfusion and T_1 by plotting the difference
59
60

1
2
3 of the means over two scanning days vs the mean. For group B, the same
4 analysis was performed using the single measurements made during each
5 session.
6
7

8 9 10 **Results:**

11 An example of a multi-slice quantitative 3D GRASE ASL perfusion data set
12 from one volunteer is shown in Figure 2. The central 8 slices are presented,
13 and clearly display the regional variations of renal perfusion. The full set of
14 parameter maps of a central slice obtained from another volunteer is shown in
15 Figure 3. Figure 4 shows an example of the ROIs used for statistical analysis.
16
17

18 Short-term repeatability study (Tables 1a and b):

19
20 **Group A:** The mean within-subject standard deviation (SD_{ws}) for the cortical
21 perfusion was $14.6 \text{ mL min}^{-1} 100 \text{ g}^{-1}$ (right kidney) and $14.2 \text{ mL min}^{-1} 100 \text{ g}^{-1}$
22 (left kidney). For both the right and left whole kidney regions, SD_{ws} was 10.1
23 $\text{mL min}^{-1} 100 \text{ g}^{-1}$.
24
25

26 Averaged perfusion results of all three scans obtained on both scanning
27 sessions had a mean value of $204 \text{ mL min}^{-1} 100 \text{ g}^{-1}$ with a CV_{ws} of 7.12 % for
28 the right cortical region and $189 \text{ mL min}^{-1} 100 \text{ g}^{-1}$ with a CV_{ws} of 7.52 % for the
29 left cortical region. The whole kidney values were $188.2 \text{ mL min}^{-1} 100 \text{ g}^{-1}$ with
30 a CV_{ws} of 5.37 % for the right and $172 \text{ mL min}^{-1} 100 \text{ g}^{-1}$ with a CV_{ws} of 5.86 %
31 for the left kidney.
32
33

34 The SD_{ws} for T_1 values were 33ms and 26ms for the right and left cortical
35 regions respectively and 14ms and 21ms for the right and left whole kidney
36 regions respectively. Averaged T_1 results of all three scans obtained on both
37 scanning sessions had a mean value of 1240ms with a CV_{ws} of 2.69 % and
38 1290ms with a CV_{ws} of 1.99 % for the right and left cortical regions
39 respectively. For the whole kidney regions, T_1 (right kidney) = 1460ms with a
40 CV_{ws} of 0.97 % and T_1 (left kidney) = 1470ms with a CV_{ws} of 1.41 %.
41
42
43
44
45

46 Long-term repeatability study:

47
48 **Group A:** Bland-Altman plots for perfusion and T_1 are shown in Figure 5. All
49 data points were contained within the limits of agreement (mean of difference
50 ± 1.96 SD of difference) marked on the plots. The largest difference between
51 sessions was seen in Volunteer 4 perfusion values ($105 \text{ mL min}^{-1} 100 \text{ g}^{-1}$ of
52 tissue for the cortical region), which is still smaller than the normal variation
53 recorded by Chasis et al. (31).
54
55

56 The mean \pm SD of the arterial transit time measurements made in all the
57 subjects in Group A were 143 ± 45 ms for the cortex and 102 ± 31 ms for the
58 whole kidney ROI, making cortical Δt significantly longer than whole kidney
59 Δt ($p < 10^{-7}$).
60

1
2
3
4 **Group B:** for the larger group (20 volunteers) mean cortical perfusion values
5 on the first and second scans were 196 and 204 ml/100gm/min respectively. A
6 Bland-Altman plot showing the between-session difference of the mean
7 perfusion (averaged over both kidneys) is shown in Figure 6. As with group
8 A, the spread of the perfusion differences were contained within the limits of
9 agreement, and the mean difference is very close to zero (-1.4 ml/100g/min).
10 The SD of the inter-session perfusion difference in this group was 62.4
11 ml/100g/min. Table 2 shows the median perfusion and T_1 values for all Group
12 B subjects in the cortical and whole kidney ROIs for both scanning sessions.
13
14
15
16

17 18 **Discussion:**

19 The aim of this study was to determine the repeatability of 3D GRASE ASL of
20 the kidney in a clinical setting. If a totally non-invasive bio-marker of renal
21 perfusion can be established, this will allow the researcher and clinician to
22 calculate the filtration fraction of each kidney. The filtration fraction is the
23 ratio of renal plasma flow to glomerular filtration, a critical parameter in
24 understanding kidney function in all disease states. The effect of medication,
25 especially those used for the treatment of hypertension and cardiac failure
26 (Angiotensin I-converting enzyme inhibitors (ACE)) on renal function will be
27 able to be monitored accurately. The potential value of a repeatable measure
28 of renal perfusion in patients following renal transplantation needs to be
29 assessed as it may provide a sensitive measure of early allograft rejection.
30
31

32 The main advantage of ASL is the ability to measure perfusion without the
33 use of an exogenous tracer. The other MR technique that measures perfusion,
34 Dynamic Contrast-Enhanced (DCE-MRI), uses the gadolinium-based contrast
35 material. Following reports of nephrogenic systemic fibrosis (NSF) after DCE-
36 MRI, strict limitations are in place when there is chronic renal insufficiency.
37 Although tracers have improved, and NSF is reported infrequently,
38 nevertheless certain nephrology groups (mainly paediatric nephrology) will
39 not allow DCE-MRI in children following renal replacement therapy. This
40 emphasises the need to assess ASL and ensure its robustness and reliability.
41
42

43 Perfusion results obtained from our healthy volunteers were consistent with
44 those found in the literature measured with modalities other than MRI (26,
45 31-33). Renal cortical perfusion values obtained in normal subjects using ASL
46 found in the literature vary varied from $213 \pm 55 \text{ mL min}^{-1} 100 \text{ g}^{-1}$ with a range
47 from 140 to $319 \text{ mL min}^{-1} 100 \text{ g}^{-1}$ (11), $245 \pm 11 \text{ mL min}^{-1} 100 \text{ g}^{-1}$ using a 3T
48 system (34), $375 \pm 54 \text{ mL min}^{-1} 100 \text{ g}^{-1}$ (23) to $407 - 456 \text{ mL min}^{-1} 100 \text{ g}^{-1}$ with
49 mean $427 \pm 20 \text{ mL min}^{-1} 100 \text{ g}^{-1}$ (15). All these publications used the simplified
50 kinetic model based on a single TI acquisition to calculate renal perfusion. We
51 chose to use the Buxton model (22), in which data from all the time intervals
52 (TIs) acquired are used to fit the model rather than using just one data point.
53
54
55
56
57
58
59
60

1
2
3
4 This will be especially important in case of renal artery stenosis for example,
5 while we expect it to play a minor role in case of unobtrusive arterial flow. On
6 the other hand, the pattern of flow, including blood velocity and arterial
7 pulsatility might be different in transplanted kidneys and other disease-
8 affected kidneys, and as such we think that a multi-TI approach would be
9 preferable a priori, even at the cost of a slightly increased scan time.
10 Alternatively, a single TI approach using Q2TIPS (or the recently developed
11 QUIPSS II with window-sliding saturation sequence (Q2WISE)) to reduce the
12 sensitivity to transit times may be a favourable option (19, 35). While offering
13 a better overall efficiency by focusing on the region of the ASL inflow curve
14 with the highest signal change, Q2TIPS and Q2WISE rely on certain
15 haemodynamic assumptions being satisfied (20). In some situations, it will be
16 difficult to know in advance if this is the case. Therefore, the optimum ASL
17 acquisition scheme will depend on the details of any particular application.
18
19
20
21
22
23

24 In this study, we used background suppression to reduce artefacts and noise
25 from the background tissue signal, and respiratory gating to ensure that the
26 labelling pulses were consistently applied at the same point in the respiratory
27 cycle. While background suppression is generally accepted as a method to
28 significantly improve the quality of ASL data (28, 36), it has also been
29 reported that it can decrease the reproducibility of the measurement (23). In
30 our experience, despite the small loss of labelling efficiency caused by the use
31 of background suppression pulses, the reduced level of noise present in our
32 3D acquisitions meant that background suppression improved the precision
33 of the ASL blood flow measurements. The usefulness of respiratory gating is
34 also an open question; while it has been used in some other studies (e.g. (37)),
35 it has also been shown to offer no clear benefit over free breathing
36 acquisitions, particularly when image registration is used (23, 36). In this
37 study, given the multi-TI acquisition strategy, images were acquired at a
38 range of different times after the labelling pulse, and so the method may be
39 susceptible to motion-related problem as the kidney position varies during
40 the respiratory cycle. In the future, we intend to investigate the benefit of
41 using motion correction algorithms to improve measurement precision. The
42 volumetric 3D image acquisition scheme used here is particularly suitable for
43 this type of post-processing correction.
44
45
46
47
48
49
50
51
52

53 Several studies have also investigated the repeatability of ASL measurements
54 in the kidney. Karger et al. (11) used two volunteers scanned twice and 1
55 scanned 3 times, from which they obtained an average reproducibility error of
56 11% using a FAIR-UFLARE sequence. For two of these volunteers, coronal
57 slices were used while transverse slices were obtained for the other one. The
58 present study shows repeated measurements in several volunteers acquired
59 in exactly the same orientation and with the same protocol. Also using a
60

1
2
3
4 single shot fast spin echo readout, but in this case with a pCASL labelling
5 scheme, Robson et al. (36) showed test-retest repeatability between sessions
6 one week apart was between 7% and 23% (depending on the type of
7 background suppression and breathing strategy used) and within session
8 variability was 8% for strong background suppression and timed breathing.
9 Gardener et al. (23) used both TrueFISP and EPI readout modules in
10 combination with FAIR labelling and showed test-retest reproducibility
11 between sessions of better than 10% for all realigned free-breathing, triggered,
12 and breath-hold data sets acquired in the absence of BS. Interestingly, the
13 background-suppressed free breathing measurements showed a higher
14 variability (up to 20%). Lastly, Artz *et al.* have recently investigated the
15 reproducibility of ASL measurements in native and transplanted kidneys
16 using FAIR TrueFISP (37). In the native kidneys, they found intra-session CVs
17 of ~5% and inter-session CVs of 11-13%. In the study presented here, we have
18 assessed the reproducibility of a different image acquisition module
19 (segmented 3D GRASE) which allows for rapid volumetric imaging of the
20 whole kidney. We have also used a more advanced multi-TI acquisition
21 scheme, which allows fitting of the ASL kinetic model and should provide
22 more accurate estimates of perfusion. Nevertheless, this study adds to the
23 growing weight of evidence showing that ASL is a robust technique for
24 measuring renal blood flow and is a viable alternative to DCE for clinical
25 applications.
26
27
28
29
30
31
32
33

34
35 As expected, the whole kidney perfusion values measured in $\text{mL min}^{-1} 100 \text{ g}^{-1}$
36 of tissue were consistently lower than their respective cortical values.
37 Variation in perfusion in healthy subjects is known to vary even over the
38 course of a day in the same person. Chasis et al. (31) found an intra-individual
39 variation of around $140 \text{ mL min}^{-1} 100 \text{ g}^{-1}$ of tissue in their study of 15 healthy
40 volunteers. In the volunteer studies presented here, mean perfusion values
41 between individuals varied from 90 to $303 \text{ mL min}^{-1} 100 \text{ g}^{-1}$ of tissue.
42 However, little variation was seen in the same individual. As there was a
43 wide age range, weight and height between the volunteers, these findings are
44 expected. The within-subject CVs obtained were small compared to those
45 obtained with other techniques (33). Also, in group A, a maximum SD_{ws} of 15
46 $\text{mL min}^{-1} 100 \text{ g}^{-1}$ of tissue is within the physiological variation measured in
47 previous studies (31). These results imply that there was minimal variation
48 between the three acquisitions on both the first and second scanning
49 occasions, showing that the technique is repeatable over a short period of
50 time. Bland Altman plots were used to assess the variability between the two
51 scanning sessions shows all data points contained within the limits of
52 agreement (mean of difference $\pm 1.96 \text{ SD}$ of difference) marked on the plots.
53 The largest difference between sessions was $107 \text{ mL min}^{-1} 100 \text{ g}^{-1}$ of tissue for
54 the cortical region, which is still smaller than the normal variation recorded in
55
56
57
58
59
60

1
2
3
4
5
6
7
8
9
10
11
12
13
14
15
16
17
18
19
20
21
22
23
24
25
26
27
28
29
30
31
32
33
34
35
36
37
38
39
40
41
42
43
44
45
46
47
48
49
50
51
52
53
54
55
56
57
58
59
60

Chasis et al. (31). Arterial transit time values were significantly longer in the cortex compared to the whole kidney, though both were shorter than might have been expected from previous work (*e.g.* (9)). This is most likely related to the relative geometry of the labelling and imaging slabs used in this work (the inversion region is immediately adjacent to the imaging volume), and the absence of vascular crusher gradients in the 3D GRASE acquisition scheme.

Conclusion:

In this work we assessed the repeatability of renal ASL with the aim of establishing its potential for routine clinical use. This preliminary study shows that ASL parameters are repeatable, over a short and long period of time, implying that ASL can be reliably used to assess patients longitudinally. Critically, ASL provides a measure for renal perfusion, which is one of the main functions of the kidney. The only other way one can obtain this parameter using MR is to use contrast enhanced imaging techniques, unavailable to most patients suffering from kidney insufficiency because of the risk of Nephrogenic Systemic Fibrosis (NSF) linked to the administration of gadolinium. In addition, ASL is also fast and of minimal burden to the patients and hence can be incorporated into routine anatomical MR scans.

Acknowledgements:

The authors would like to thank Dr Martin King for his valuable discussion, advice and help with the statistical analysis presented in this study. We would also like to thank Dr Matthias Günther for providing the 3D GRASE ASL pulse sequence.

The authors acknowledge Kidney Research UK for part-funding this study of ASL in volunteers.

References

1. Neimatallah MA, Dong Q, Schoenberg SO, Cho KJ, Prince MR. (1999) Magnetic resonance imaging in renal transplantation. *J Magn Reson Imaging* 10(3):357-368.
2. Szolar DH, Preidler K, Ebner F, Kammerhuber F, Horn S, Ratschek M, Ranner G, Petritsch P, Horina JH. (1997) Functional magnetic resonance imaging of human renal allografts during the post-transplant period: preliminary observations. *Magn Reson Imaging* 15(7):727-735.
3. Haufe SE, Riedmuller K, Haberkorn U. (2006) Nuclear medicine procedures for the diagnosis of acute and chronic renal failure. *Nephron Clin Pract* 103(2):c77-c84.
4. Peters AM, Brown J, Hartnell GG, Myers MJ, Haskell C, Lavender JP. (1987) Non-invasive measurement of renal blood flow with ^{99m}Tc DTPA: comparison with radiolabelled microspheres. *Cardiovasc Res* 21(11):830-834.
5. Golay X, Hendrikse J, Lim TC. (2004) Perfusion imaging using arterial spin labeling. *Top Magn Reson Imaging* 15(1):10-27.
6. Petersen ET, Zimine I, Ho YC, Golay X. (2006) Non-invasive measurement of perfusion: a critical review of arterial spin labelling techniques. *Br J Radiol* 79(944):688-701.
7. Buxton RB. (2002) Introduction to Functional Magnetic Resonance Imaging. Cambridge University Press
8. Martirosian P, Boss A, Schraml C, Schwenzer NF, Graf H, Claussen CD, Schick F. (2010) Magnetic resonance perfusion imaging without contrast media. *Eur J Nucl Med Mol Imaging* 37 Suppl 1:S52-S64.
9. Roberts DA, Detre JA, Bolinger L, Insko EK, Lenkinski RE, Pentecost MJ, Leigh JS, Jr. (1995) Renal perfusion in humans: MR imaging with spin tagging of arterial water. *Radiology* 196(1):281-286.
10. Chen Q, Siewert B, Bly BM, Warach S, Edelman RR. (1997) STAR-HASTE: perfusion imaging without magnetic susceptibility artifact. *Magn Reson Med* 38:404-408.
11. Karger N, Biederer J, Lusse S, Grimm J, Steffens J, Heller M, Gluer C. (2000) Quantitation of renal perfusion using arterial spin labeling with FAIR-UFLARE. *Magn Reson Imaging* 18(6):641-647.
12. Martirosian P, Klose U, Mader I, Schick F. (2004) FAIR True-FISP perfusion imaging of the kidneys. *Magn Reson Med* 51:353-361.
13. De Bazelaire C, Rofsky NM, Duhamel G, Michaelson MD, George D, Alsop DC. (2005) Arterial spin labeling blood flow magnetic resonance imaging for

- 1
2
3 the characterization of metastatic renal cell carcinoma(1). Acad Radiol
4 12(3):347-357.
5
6
7 14. Fenchel M, Martirosian P, Langanke J, Giersch J, Miller S, Stauder NI, Kramer
8 U, Claussen CD, Schick F. (2006) Perfusion MR imaging with FAIR true FISP
9 spin labeling in patients with and without renal artery stenosis: initial
10 experience. Radiology 238(3):1013-1021.
11
12 15. Artz NS, Sadowski EA, Wentland AL, Grist TM, Seo S, Djamali A, Fain SB.
13 (2011) Arterial spin labeling MRI for assessment of perfusion in native and
14 transplanted kidneys. Magn Reson Imaging 29(7):74-82.
15
16 16. Lanzman RS, Wittsack HJ, Martirosian P, Zgoura P, Bilk P, Kropil P, Schick F,
17 Voiculescu A, Blondin D. (2010) Quantification of renal allograft perfusion
18 using arterial spin labeling MRI: initial results. Eur Radiol 20(6):1485-1491.
19
20 17. Pedrosa I, Alsop DC, Rofsky NM. (2009) Magnetic resonance imaging as a
21 biomarker in renal cell carcinoma. Cancer 115(10 Suppl):2334-2345.
22
23 18. Kim SG. (1995) Quantification of relative cerebral blood flow change by flow-
24 sensitive alternating inversion recovery (FAIR) technique: application to
25 functional mapping. Magn Reson Med 34:293-301.
26
27 19. Song R, Loeffler RB, Hillenbrand CM. (2010) Improved renal perfusion
28 measurement with a dual navigator-gated Q2TIPS fair technique. Magn Reson
29 Med 64(5):1352-1359.
30
31 20. Wong EC, Buxton RB, Frank LR. (1998) Quantitative imaging of perfusion
32 using a single subtraction (QUIPSS and QUIPSS II). Magn Reson Med 39:702-
33 708.
34
35 21. Dobbs, M. S., Woodhouse, N., Parker, G. J., and Naish, J. H. (2010) Renal ASL
36 using multiple inversion time, free breathing STAR-HASTE technique at 3T
37 [abstract]. In: Proc 18th Meeting of ISMRM p2676.
38
39 22. Buxton RB, Frank LR, Wong EC, Siewert B, Warach S, Edelman RR. (1998) A
40 general kinetic model for quantitative perfusion imaging with arterial spin
41 labeling. Magn Reson Med 40(3):383-396.
42
43 23. Gardener AG, Francis ST. (2010) Multislice perfusion of the kidneys using
44 parallel imaging: image acquisition and analysis strategies. Magn Reson
45 Imaging 63(6):1627-1636.
46
47 24. Gunther M, Oshio K, Feinberg DA. (2005) Single-shot 3D imaging techniques
48 improve arterial spin labeling perfusion measurements. Magn Reson Med
49 54(2):491-498.
50
51 25. Freeman R. (1997) A Handbook of Nuclear Magnetic Resonance.
52 Longman Limited, London; p275.
53
54 26. Regan MC, Young LS, Geraghty J, Fitzpatrick JM. (1995) Regional renal blood
55 flow in normal and disease states. Urol Res 23(1):1-10.
56
57
58
59
60

- 1
 - 2
 - 3
 - 4
 - 5
 - 6
 - 7
 - 8
 - 9
 - 10
 - 11
 - 12
 - 13
 - 14
 - 15
 - 16
 - 17
 - 18
 - 19
 - 20
 - 21
 - 22
 - 23
 - 24
 - 25
 - 26
 - 27
 - 28
 - 29
 - 30
 - 31
 - 32
 - 33
 - 34
 - 35
 - 36
 - 37
 - 38
 - 39
 - 40
 - 41
 - 42
 - 43
 - 44
 - 45
 - 46
 - 47
 - 48
 - 49
 - 50
 - 51
 - 52
 - 53
 - 54
 - 55
 - 56
 - 57
 - 58
 - 59
 - 60
27. Cheong B, Muthupillai R, Rubin MF, Flamm SD. (2007) Normal values for renal length and volume as measured by magnetic resonance imaging. *Clin J Am Soc Nephrol* 2(1):38-45.
27. Ye FQ, Frank JA, Weinberger DR, McLaughlin AC. (2000) Noise reduction in 3D perfusion imaging by attenuating the static signal in arterial spin tagging (ASSIST). *Magn Reson Med* 44(1):92-100.
29. Bland JM, Altman DG. (1996) Measurement error. *Brit Med J* 313(7059):744.
30. Bland JM, Altman DG. (1986) Statistical methods for assessing agreement between two methods of clinical measurement. *Lancet* 1(8476):307-310.
31. Chasis H, Ranges HA, Goldring W, Smith HW. (1938) The control of renal blood flow and glomerular filtration in normal man. *J Clin Invest* 17(5):683-697.
32. Ladefoged J. (1966) Measurements of the renal blood flow in man with the 133 xenon wash-out technique. A description of the method. *Scand J Clin Lab Invest* 18(3):299-315.
33. Miles KA. (1991) Measurement of tissue perfusion by dynamic computed tomography. *Br J Radiol* 64(761):409-412.
34. Kiefer C, Schroth G, Gralla J, Diehm N, Baumgartner I, Husmann M. (2009) A feasibility study on model-based evaluation of kidney perfusion measured by means of FAIR prepared true-FISP arterial spin labeling (ASL) on a 3-T MR scanner. *Acad Radiol* 16(1):79-87.
35. Song R, Loeffler RB, Hillenbrand CM. (2011) QUIPSS II with window-sliding saturation sequence (Q2WISE). *Magn Reson Med* Epub ahead of print (doi: 10.1002/mrm.23093)
36. Robson PM, Madhuranthakam AJ, Dai W, Pedrosa I, Rofsky NM, Alsop DC. (2009) Strategies for reducing respiratory motion artifacts in renal perfusion imaging with arterial spin labeling. *Magn Reson Med* 61(6):1374-1387.
37. Artz NS, Sadowski EA, Wentland AL, Djamali A, Grist TM, Seo S, Fain SB. (2011) Reproducibility of renal perfusion MR imaging in native and transplanted kidneys using non-contrast arterial spin labeling. *J Magn Reson Imaging* 33(6):1414-1421.

Figure Legends

Figure 1 (a) schematic pulse sequence diagram of 3D GRASE FAIR ASL sequence. (b) Transverse TrueFISP image showing the position of two kidneys and aorta. The imaging and inversion slabs were placed on top of each other and include both kidneys. Care was taken not to include the aorta in this region, so that inflowing arterial blood was not inverted by the slice-selective inversion.

Figure 2 Multi-slice renal perfusion maps of the central 8 slices of one volunteer. Images have been masked based on M_0 values to reduce noise from tissue outside the kidneys.

Figure 3 Typical ASL parameter maps: a) longitudinal relaxation time (T_1); b) arterial transit time (Δt); c) equilibrium magnetisation (M_0); and d) perfusion

Figure 4 A typical a) cortical and b) whole kidney region of interest.

Figure 5 Bland Altman plots for inter-session variability in Group A of (a) cortical perfusion and (b) longitudinal relaxation time (T_1)

Figure 6 Bland Altman plots for inter-session cortical perfusion variability in Group B

Tables 1a and b: Columns titled Mean \pm SD list the mean of the 3 repeats on each day for Group A i.e. the mean of 2 slices for each kidney for each repeat and the Standard Deviation (SD) calculated taking the mean of the 2 slices for each repeat on a particular day. The coefficient of variation (CV) was calculated by dividing the SD by the mean and multiplying by 100.

(a) Cortical values:

	Day	Volunteer 1		Volunteer 2		Volunteer 3		Volunteer 4		Volunteer 5	
		Mean \pm SD	CV	Mean \pm SD	CV	Mean \pm SD	CV	Mean \pm SD	CV	Mean \pm SD	CV
Perfusion (mL min ⁻¹ 100 g ⁻¹)	1	160 \pm 4.79	3.07	191 \pm 23.1	12.1	192 \pm 14.3	7.13	198 \pm 9.80	4.96	202 \pm 24.2	12.0
	2	135 \pm 5.63	4.17	206 \pm 16.8	8.29	204 \pm 3.70	1.82	303 \pm 10.3	3.40	175 \pm 8.72	4.92
T ₁ (ms)	1	1290 \pm 7.3	0.57	1220 \pm 21	1.76	1210 \pm 67	5.79	1260 \pm 12	11.5	1290 \pm 15	1.19
	2	1180 \pm 26	2.24	1270 \pm 33	2.62	1330 \pm 4.5	0.34	1360 \pm 4.1	0.29	1250 \pm 23	1.78

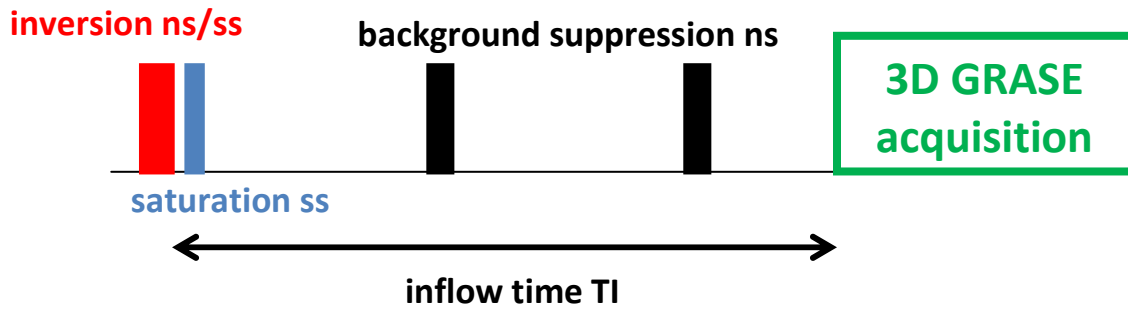
(b) Whole kidney values:

	Day	Volunteer 1		Volunteer 2		Volunteer 3		Volunteer 4		Volunteer 5	
		Mean \pm SD	CV	Mean \pm SD	CV	Mean \pm SD	CV	Mean \pm SD	CV	Mean \pm SD	CV
Perfusion (mL min ⁻¹ 100 g ⁻¹)	1	164 \pm 2.92	1.69	166 \pm 15.3	9.16	177 \pm 4.81	2.67	166 \pm 6.73	4.05	200 \pm 21.9	10.9
	2	141 \pm 2.01	1.44	176 \pm 9.61	5.50	185 \pm 2.75	1.50	258 \pm 5.56	2.15	169 \pm 4.86	2.81
T ₁	1	1475 \pm 20	1.33	1401 \pm 5.5	0.36	1480 \pm 14	0.90	1460 \pm 5.0	0.34	1450 \pm 13	0.91
	2	1420 \pm 13	0.92	1470 \pm 13	0.89	1520 \pm 6.9	0.45	1510 \pm 5.9	0.39	1470 \pm 33	2.17

Table 2: Median \pm SD of data obtained on Day 1 and Day 2 for Group B.

	Perfusion (mL min ⁻¹ 100 g ⁻¹)		T ₁ (ms)	
	Cortex	Whole kidney	Cortex	Whole kidney
Day 1	178 \pm 40.7	147 \pm 30.8	1345 \pm 119	1515 \pm 131
Day 2	187 \pm 45.6	156 \pm 39.5	1341 \pm 154	1499 \pm 171

(a)



(b)

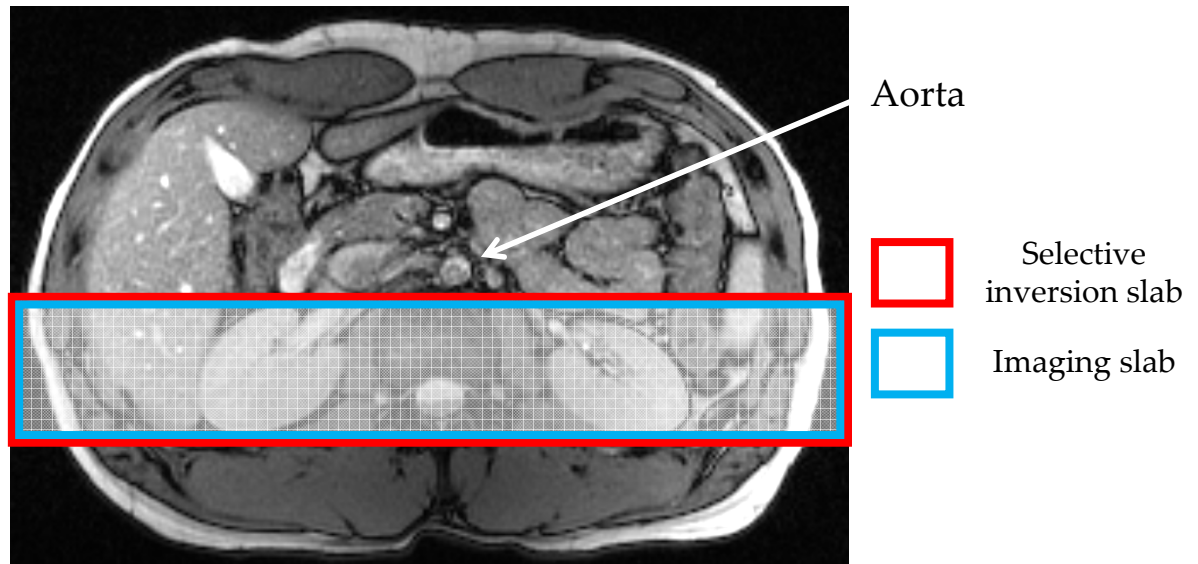


Figure 1 (a) schematic pulse sequence diagram of 3D GRASE FAIR ASL sequence. (b) Transverse TrueFISP image showing the position of two kidneys and aorta. The imaging and inversion slabs were placed on top of each other and include both kidneys. Care was taken not to include the aorta in this region, so that inflowing arterial blood was not inverted by the slice-selective inversion.

1
2
3
4
5
6
7
8
9
10
11
12
13
14
15
16
17
18
19
20
21
22
23
24
25
26
27
28
29
30
31
32
33
34
35
36
37
38
39
40
41
42
43
44
45
46
47
48
49
50
51
52
53
54
55
56
57
58
59
60

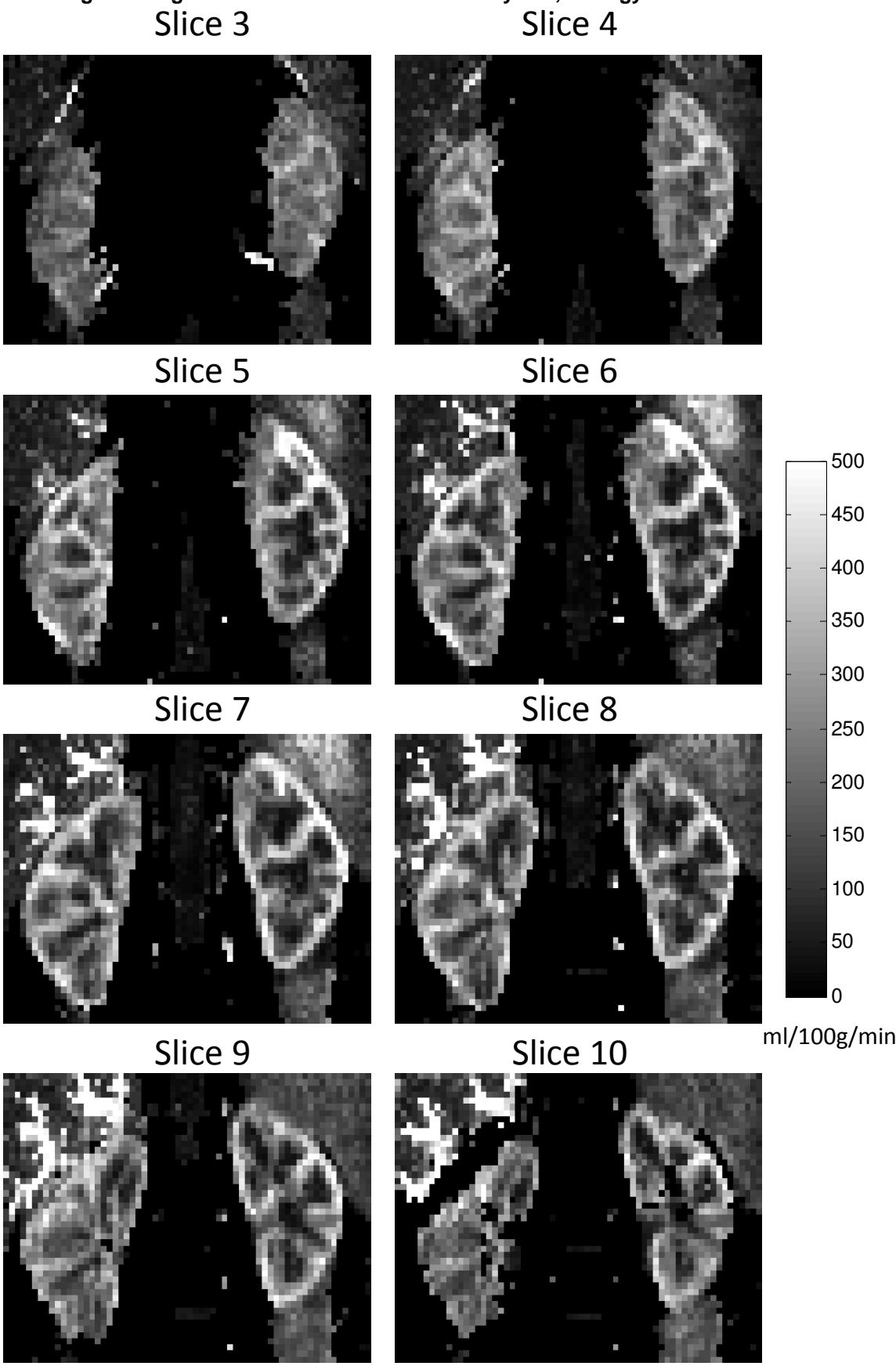


Figure 2 Multi-slice renal perfusion maps of the central 8 slices of one volunteer. Images have been masked based on M_0 values to reduce noise from tissue outside the kidneys.

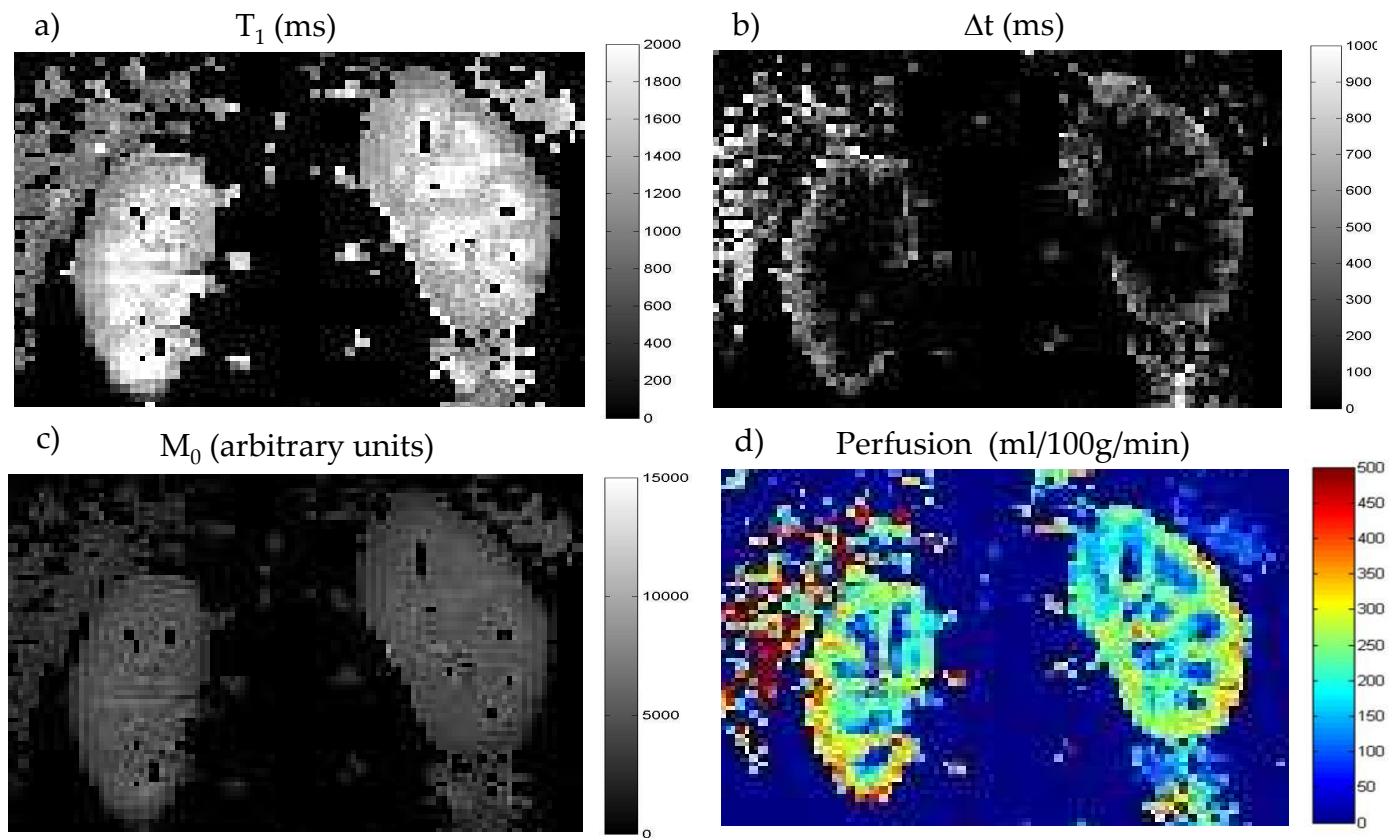


Figure 3 Typical ASL parameter maps: a) longitudinal relaxation time (T_1); b) arterial transit time (Δt); c) equilibrium magnetisation (M_0); and d) perfusion

1
2
3
4
5
6
7
8
9
10
11
12
13
14
15
16
17
18
19
20
21
22
23
24
25
26
27
28
29
30
31
32
33
34
35
36
37
38
39
40
41
42
43
44
45
46
47
48
49
50
51
52
53
54
55
56
57
58
59
60

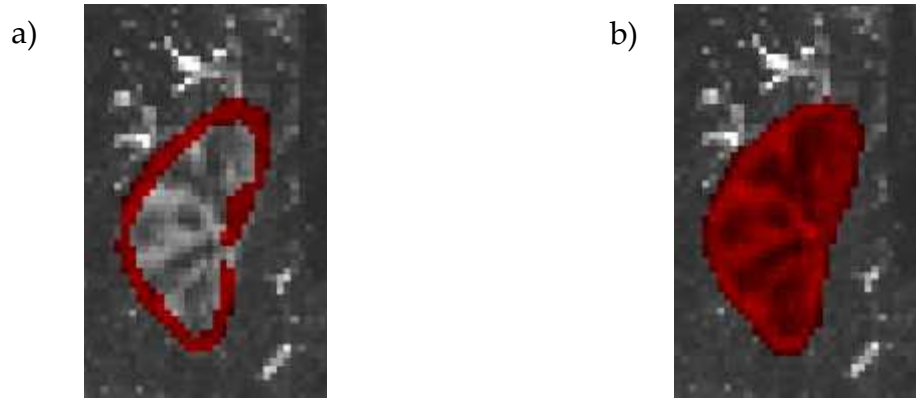


Figure 4 A typical a) cortical and b) whole kidney region of interest.

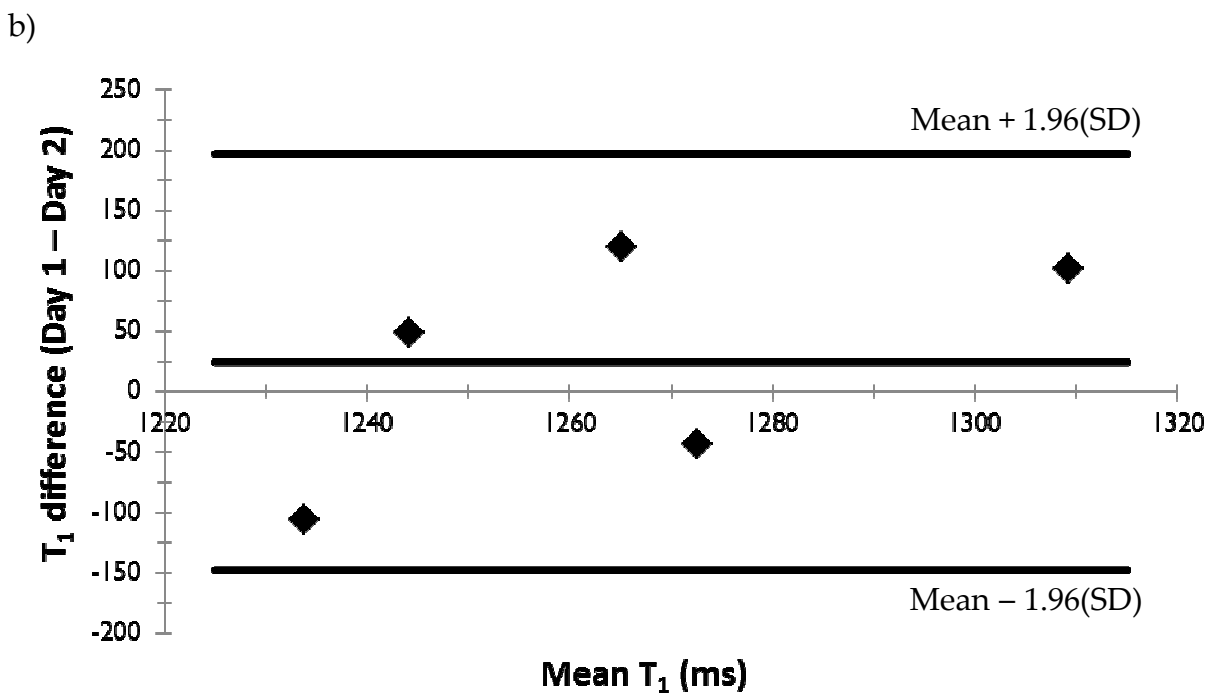
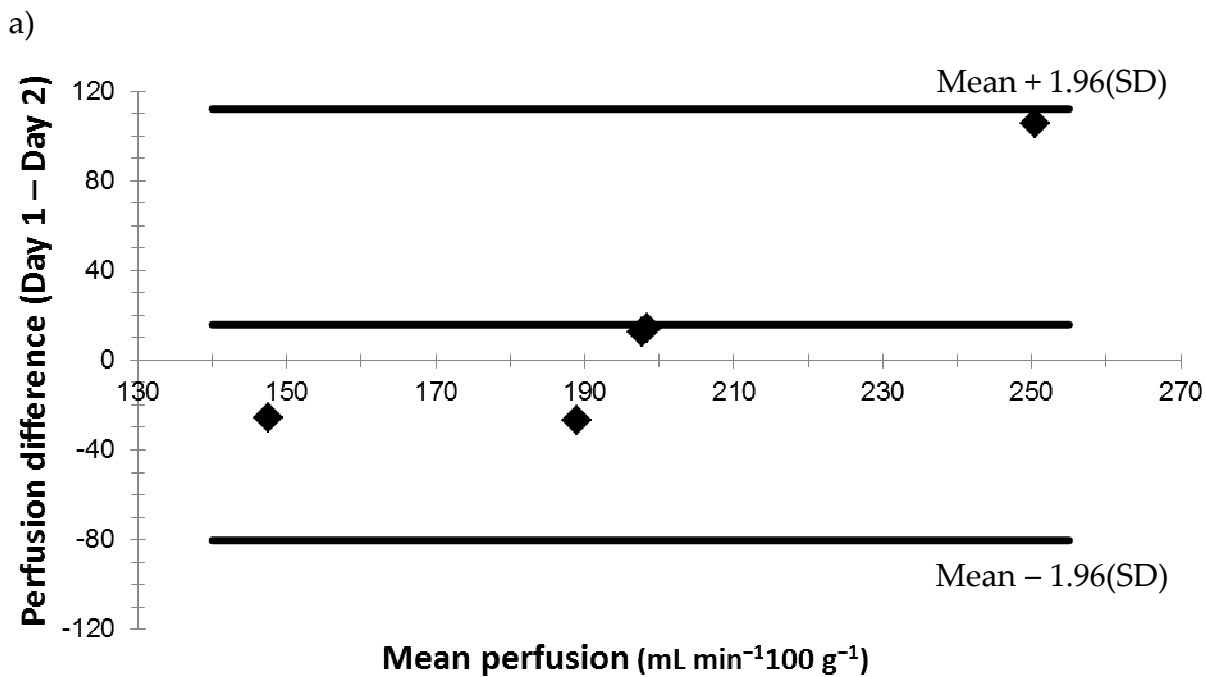


Figure 5 Bland Altman plots for inter-session variability in Group A of (a) cortical perfusion and (b) longitudinal relaxation time (T_1)

1
2
3
4
5
6
7
8
9
10
11
12
13
14
15
16
17
18
19
20
21
22
23
24
25
26
27
28
29
30
31
32
33
34
35
36
37
38
39
40
41
42
43
44
45
46
47
48
49
50
51
52
53
54
55
56
57
58
59
60

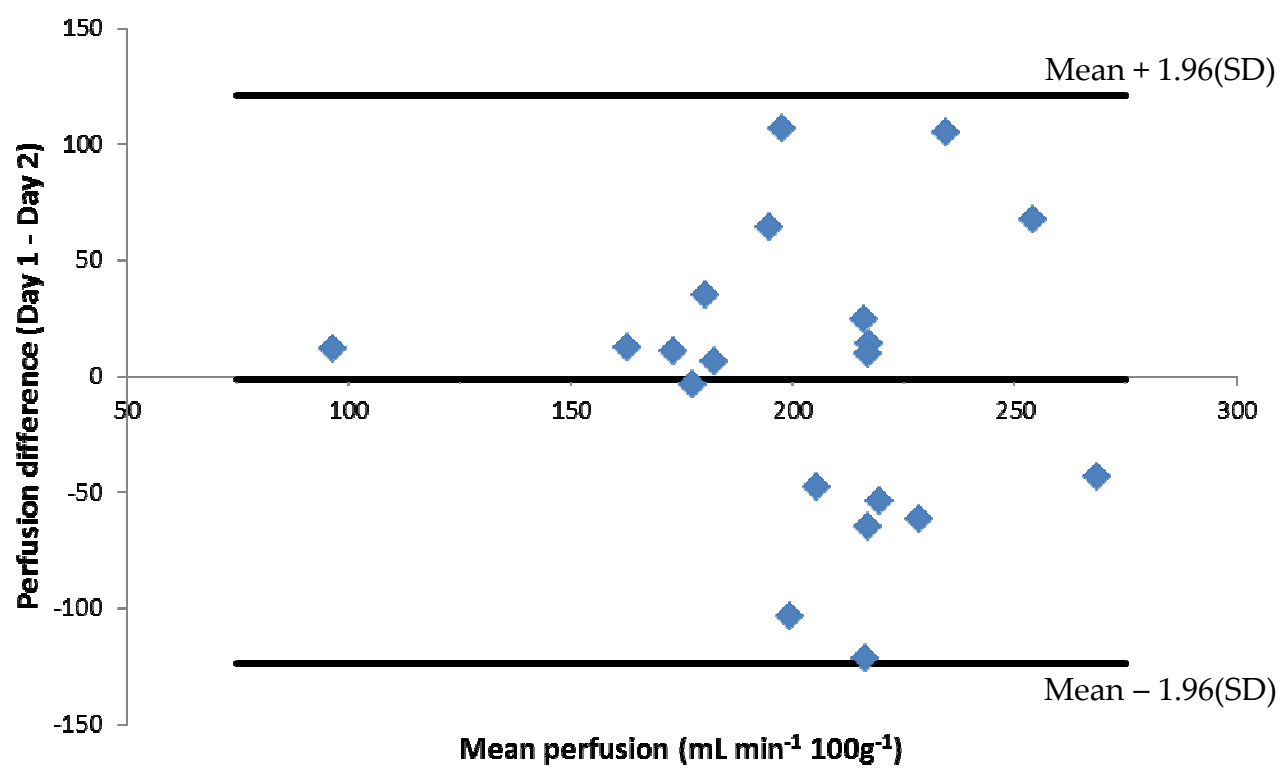


Figure 6 Bland Altman plots for inter-session cortical perfusion variability in Group B